

1 **High-resolution automated detection of headwater streambeds for large watersheds**

2 **Francis Lessard^{1,2,3}, Naïm Perreault^{1,2}, Sylvain Jutras^{1,2,3}**

3 ¹ Department of Wood and Forest Science, Université Laval, 2405 rue de la Terrasse, G1V
4 0A6, Québec, QC, Canada

5 ² Centre d'étude de la forêt, Université Laval, 2405 rue de la Terrasse, G1V 0A6, Québec,
6 QC, Canada

7 ³ CentrEau - Water Research Centre, Université Laval, 1065 avenue de la Médecine, G1V
8 0A6, Québec, QC, Canada

9

10 **Corresponding author:** Francis Lessard, francis.lessard.3@ulaval.ca

11 **Present address:** Pavillon Abitibi-Price, 2405 rue de la Terrasse, G1V 0A6, Québec, QC,
12 Canada

13

14 **Keywords:** LiDAR, Streambed, Headwater stream, Remote sensing

15 ~~Abstract: Streams are defined by the presence of a streambed, which is a linear~~
16 ~~depression where water flows between discernible banks. The upstream~~
17 ~~boundary of a stream is called a channel head.~~**Abstract:** Headwater streams,
18 which are small streams at the top of a watershed, account for the majority of
19 the total length of streams, yet their exact locations are still not well known.
20 For years, many algorithms were used to produce hydrographic networks that
21 represent headwater streams with varying degrees of accuracy. Although
22 digital elevation models derived from LiDAR have significantly improved
23 headwater stream detection, the performance of the algorithms [▲]~~on landscapes~~
24 with different ~~geomorphie~~geomorphologic characteristics remains unclear.
25 Here, we address this issue by testing different combinations of algorithms
26 using classification trees. Homogeneous hydrological processes were
27 identified through ~~hydrological classification.~~Quaternary deposits. The results
28 showed that in shallow soil that mainly consists of till deposits, the use of
29 algorithms that ~~recreate~~simulate the surface runoff process provide the best
30 explanation for the presence of a streambed. In contrast, streambeds in thick
31 soil with high infiltration rates were primarily explained by a small-scale
32 incision algorithm. Furthermore, the use of an iterative process that
33 ~~recreate~~simulate water diffusion made it possible to ~~more accurately~~
34 streambeds more accurately than all other methods tested, regardless of the
35 hydrological classification. The method developed in this paper shows the
36 importance of considering hydrological processes when aiming to identify
37 headwater streams.

a mis en forme : Police :Italique

38 ~~223~~197 words

39

40 1. Introduction

41 Streams are characterized by the presence of natural linear depressions, called streambeds.

42 Streambeds, which are ~~mostly~~ formed by fluvial processes, consist of a bed floor and banks,

43 and are identified morphologically. The upstream location of a streambed is generally

44 recognized as being the beginning of a stream and is referred as the channel head. At times,

45 streambeds can be discontinuous or diffuse, leading to subjective identification of

46 streambeds in the field and influence the determined location of the surveyed channel head

47 (Dietrich and Dunne, 1993; Wohl, 2018). On a large scale, headwater streams are

48 extremely important to maintain natural hydrological processes. Indeed, they are

49 representing about two-thirds of the total length of streams in a large watershed (Leopold

50 et al., 1964). Because they have varied ecosystems that include ecotones, headwater

51 streams support rich and diverse fauna and flora (Meyer et al., 2007). In addition,

52 headwater streams provide many ecological services to humans, including good quality

53 drinking water (Alexander et al., 2007; Freeman et al., 2007) and flood control (St-Hilaire

54 et al., 2016). Creed et al. (2017) estimated that for 2.9 million km of headwater streams in

55 the United States, 15.7 trillion US \$ in ecological services are provided annually.

56 Cartographic information on headwater streams at national or provincial scales are largely

57 derived from photointerpretation of stereoscopic aerial photography. This is the main

58 method used for the Géobase du réseau hydrographique du Québec (GRHQ) in Quebec

59 province, Canada. This geodatabase combines and standardizes several sources of

60 hydrographic data, covering an area of 154 million hectares and representing millions of

61 hydrographic features identified from aerial photos. Unfortunately, this method, as other
62 National Hydrography Dataset (NHD) underestimates the true length of streams and is
63 especially inaccurate when identifying where streams begin and where they become
64 permanent-perennial (Hafen et al., 2020). Streambeds are often imperceptible on
65 stereoscopic images where only the wide valleys are evident (Montgomery and Dietrich,
66 1994).

67 Other methods based on a digital elevation model (DEM) have been used for several years
68 to detect streams. These methods, used to produce hydrographic networks, can be divided
69 into two main categories: channel initiation and valley recognition (Lindsay, 2006). The
70 channel initiation method can be used to identify the potential locations of streambeds by
71 thresholding a flow accumulation raster by a minimum drainage area (Band, 1986; Fairfield
72 and Leymarie, 1991; Jenson and Dominique, 1988; O'Callaghan and Mark, 1984). Valley
73 recognition can be used to detect streambeds locally through a moving window that
74 identifies specific pattern depending on the algorithm used (Passalacqua et al., 2012;
75 Peucker and Douglas, 1975; Tribe, 1992). Other authors have attempted to include the
76 slope to a flow accumulation raster in order to produce more explicit models (Elmore et
77 al., 2013; Henkle et al., 2011; James et al., 2010; Montgomery and Fofoula-Georgiou,
78 1993). These methods have been widely used with coarse resolution DEMs (greater than
79 10 m) that have generally been derived from aerial photos.

80 High resolution geospatial data from Light Detection and Ranging (LiDAR) technology
81 allows for more accurate detection of headwater streams. ~~These data have recently been~~
82 ~~made available over large areas, by~~ providing topographic data on the microtopography
83 under the forest canopy and allowing the creation of DEMs with unprecedented accuracy

84 ([Murphy et al., 2008](#); [Wulder et al., 2008](#)). The hydrographic networks generated with
85 these new DEMs are much more accurate than those derived from photointerpretation or
86 those produced from DEMs with a coarser resolution ([Goulden et al., 2014](#)). ~~These DEMs~~
87 ~~allow for the subdivision of a larger number of small, previously undetected watersheds,~~
88 ~~thus generating multiple headwater streams, and consequently, many branches.~~ Various
89 authors have attempted to use these DEMs to improve the accuracy of hydrographic
90 networks and the position of channel heads. LiDAR-derived DEMs have been used to
91 detect streams both locally ([Cho et al., 2011](#); [James et al., 2007](#)) and through channel
92 initiation using a drainage area threshold ([Murphy et al., 2008](#); [Persendt and Gomez, 2016](#)).
93 ~~Other authors have attempted to include the slope to a flow accumulation raster in order to~~
94 ~~produce more explicit models ([Elmore et al., 2013](#); [Henkle et al., 2011](#); [James et al., 2010](#);~~
95 ~~[Montgomery and Foufoula-Georgiou, 1993](#)).~~ While ~~these methods~~ LiDAR-derived DEMs
96 are more representative of the local impact of water, they still ignore the heterogeneity of
97 ~~an area and the many other elements~~ Quaternary deposits that can affect bedstreambed
98 formation. Among other things, some authors noted the sensitivity of local flow direction
99 to the elevation error of the DEM ([Hengl et al., 2010](#); [O'Neil and Shortridge, 2013](#);
100 [Schwanghart and Heckmann, 2012](#)). DEMs derived from LiDAR data were also used to
101 quantify the variability of ~~permanent~~ perennial stream flow lengths, although those studies
102 did not specify where the streambed begins ([Jensen et al., 2018, 2019](#); [Van Meerveld et al.,](#)
103 [2019](#)). To the best of our knowledge, no study has addressed streambed detection using
104 LiDAR data while considering both channel initiation and valley recognition methods
105 ([Heine et al., 2004](#)) on a territory with heterogeneous ~~territory at the geomorphological~~
106 ~~level~~ geomorphologic characteristics, such as slope or Quaternary deposits ([Wu et al.,](#)

107 2021). Also, no study uses such a large ~~validation~~calibration database from real
108 observations acquired in the field.

109 The main objective of ~~our~~this study is to detect headwater streambeds at a provincial scale.

110 ~~Our~~Specific objectives are to consider hydrological processes through Quaternary deposits
111 and to use simple, well-documented streambed detection methods that can be exported to
112 different geomorphologic contexts with local calibration data. The proposed method
113 overcomes the many challenges that have limited ~~this information~~efficient streambed
114 detection in the past. These challenges include highly heterogeneous
115 ~~geomorphological~~geomorphologic characteristics (such as ~~surface~~Quaternary deposits)
116 and strong anthropization of the land, as observed in numerous agricultural watersheds
117 where headwater streams have been linearized and deepened (Couture, 2023; Sanders et
118 al., 2020).

119 2. Study areas

120 The study areas were located in the Appalachian Mountains, St. Lawrence Lowlands,
121 Southern Laurentides Highlands and Abitibi Lowlands natural provinces, according to the
122 Quebec Ecological Reference Framework (Fig. 1). This reference framework divides the
123 territory of Quebec into spatially homogeneous units at various, intertwined levels. The
124 different levels describe homogeneous units in terms of landform, spatial organization, and
125 hydrographic network configuration (Direction de l'expertise en biodiversité, 2018). The
126 diversity of the natural provinces thus selected provides a general ~~description~~representation
127 of the headwater streams in Quebec. These natural provinces have distinct hydrological
128 processes resulting from geological structure and Quaternary deposits.

129 The Southern Laurentides Highlands is mostly covered by till, the most widespread
130 surfaceQuaternary deposit in the province of Quebec (Blouin and Berger, 2004; Gosselin,
131 2002). This natural province is mountainous, with altitudes varying from 200 to 1200 m.

132 The bedrock mainly consists of gneiss. SurfaceQuaternary deposits are generally thin on
133 summits and steep slopes and thicker on valley bottoms and gentle slopes. The land in the

134 Southern Laurentides Highlands is largely forested. In the Appalachian Mountains, the

135 surfaceQuaternary deposits are somewhat similar in distribution to those in the Southern
136 Laurentides Highlands, although they are thicker in certain areas. However, the bedrock in

137 the Appalachian Mountains is sedimentary and therefore very different from the Southern

138 Laurentides Highlands. The altitude here varies from 0 to 1200 m. Unlike the Southern

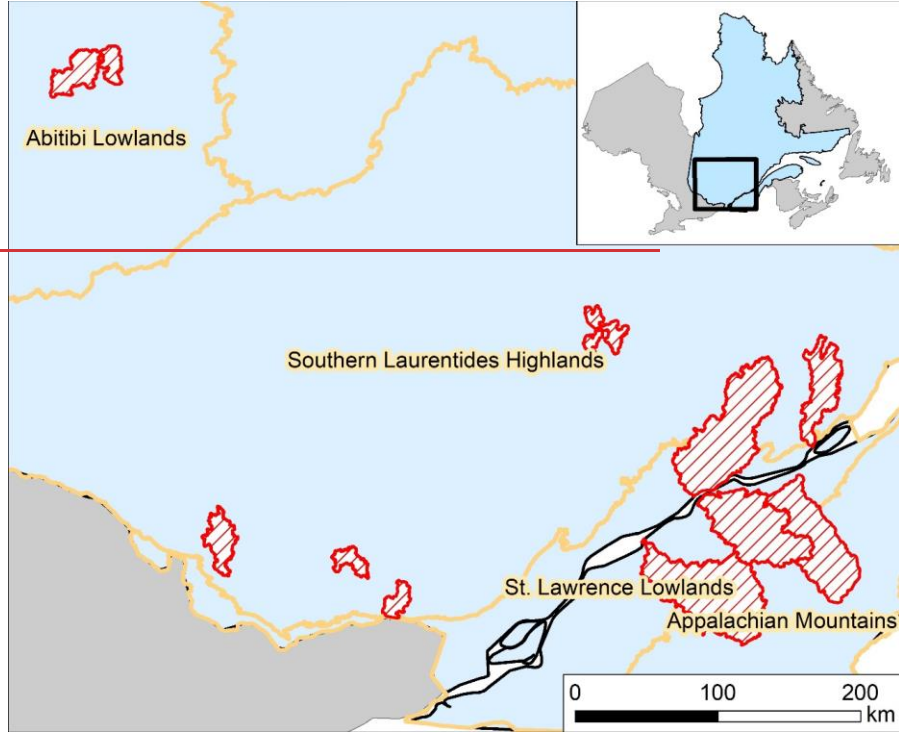
139 Laurentides Highlands, there is high anthropization of this natural province due to

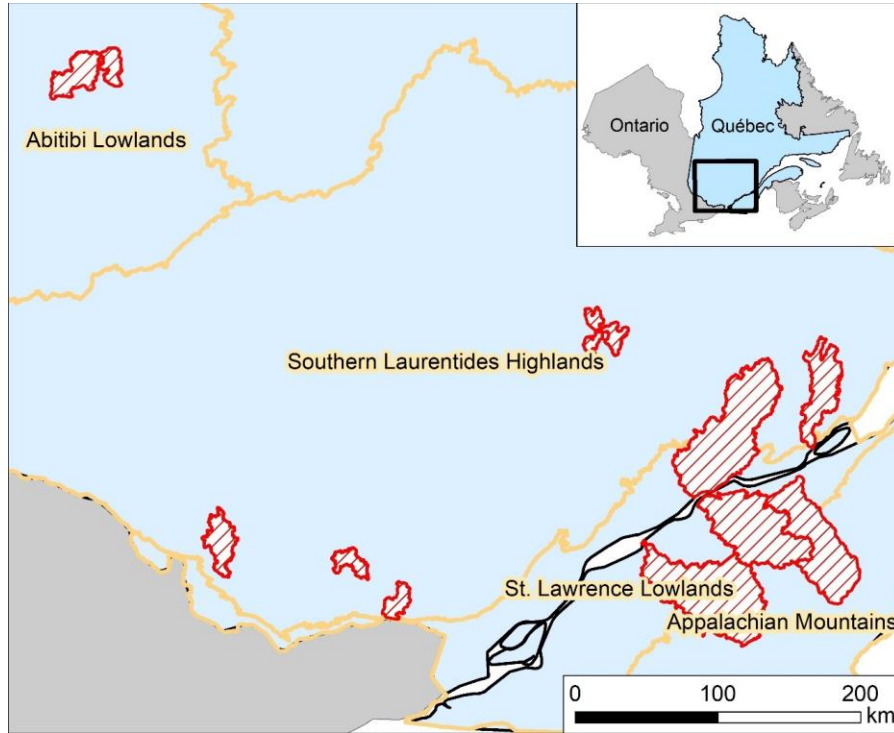
140 ~~urbanization and~~ agriculture (Gosselin, 2005a). In the St. Lawrence Lowlands, agricultural

141 activity is also widespread. The surfaceQuaternary deposits in this region are highly

142 heterogeneous and are mainly derived from marine and glaciolacustrine
143 ~~geomorphie~~geomorphologic processes. These processes lead to thick soils of sorted
144 material, including clay and sand. These, in turn, create deposits that range from
145 impermeable to very permeable. In addition to clay and sand, organic deposits are also
146 present. The elevation of the St. Lawrence Lowlands is generally less than 100 m, as it was
147 formed from the Champlain Sea during deglaciation (Gosselin, 2005b). In the Abitibi
148 Lowlands, the ~~surface~~Quaternary deposits are rather thick and consist of silt and clay.
149 These deposits were produced by marine and lacustrine invasions and are conducive to the
150 formation of large peatlands. Therefore, the area is relatively flat with altitudes varying
151 from 0 to 350 m. Where present, the bedrock is made of basalt and gneiss (Blouin and
152 Berger, 2002).

153 Precipitation is not seasonal, but rather constant throughout the year in all study areas.
154 Precipitation amounts are quite homogeneous and range from 900 mm/year to 1100
155 mm/year, except in Southern Laurentides Highlands where it can reach 1450 mm/year.
156 Approximately 20 % of the precipitation falls as snow during the cold season, except in the
157 coldest regions such as the Abitibi Lowlands and the higher altitude areas of the Southern
158 Laurentides Highlands where the proportion of snow can reach 30%. Indeed, the average
159 annual temperature of all the study areas is 3° C to 5° C, except for these two regions where
160 it is 0° C (MELCC, 2022).





162

163 **Figure 1 :** Study areas in the Appalachian Mountains, St. Lawrence Lowlands, Southern
 164 Laurentides Highlands and Abitibi Lowlands natural provinces. Red polygons represent
 165 watersheds where field surveys were carried out. [Color is not required for this figure.
 166 **Single column fitting figure.**]

167

168 **3. Methods**

169 *3.1. Field surveys*

170 Field based data collection is essential to fully understand stream flow patterns. Field
 171 surveys were conducted from 2017 to 2021 during summer periods using an EOS GNSS
 172 Arrow 100 sub-meter precision GPS. The horizontal accuracy of these devices is

173 ± 0.6 m in open areas and ± 1.2 m in forested areas (Estrada, 2017). These devices were
174 connected to rugged cell phones in order to use the ArcGIS Field Maps application to
175 integrate data collection forms as well as relevant background maps.

176 The positions of streams were recorded from downstream at drainage area generally under
177 ~~1000~~ 1 000 ha to upstream until the streambed completely disappeared. The flow regime,
178 the width of the streambed, the extent of the water occupation in the streambed and the
179 presence or the absence of a water flow were collected along the stream path to establish a
180 high level of understanding. A position was taken on the streams every 50 m or so where
181 a streambed was present, i.e. where the stream had a bed floor and banks formed by a
182 fluvial process. Other positions were also taken to identify where there was no streambed.
183 ~~These~~ This information ~~were~~ was essential for consistent calibration and validation of
184 streambeds.

185 To ensure consistent data collection, a 50 m x 50 m grid was used to determine which areas
186 should be fully surveyed. These areas were mostly located at headwater streams ~~in order~~
187 to be able to include channel heads. This procedure was essential to properly assess the
188 upstream boundary of the headwater streams and precisely record where the streambeds
189 begin, where they flow from the watershed to the ~~permanent~~ perennial stream, and where
190 they are absent.

191 3.2. Variables used for analysis

192 The geomatic manipulations were mainly performed with the ArcGIS Desktop 10.7
193 software package, including the Spatial Analyst and 3D Analysis extensions. The open-
194 source SAGA-GIS (Conrad et al., 2015) and WhiteboxTools (Lindsay, 2016a)
195 ~~software's~~ software were also used.

196 The variables used for analysis were produced from 1 m resolution DEMs of the different
197 areas. These were generated from LiDAR data ~~from~~by the MFFP (Ministère des Forêts, de
198 la Faune et des Parcs), with a density of around 2.5 points/m². LiDAR acquisitions were
199 conducted from 2016 to 2019 (Leboeuf and Pomerleau, 2015), ~~with the exception of~~except
200 ~~for~~ a few areas. The road network was carefully examined ~~in order~~to include and burn all
201 culverts that could affect the flow direction (Lessard et al., 2023). ~~Hydrographie~~Indeed,
202 ~~hydrographic~~ networks are greatly affected by deviations caused by the embankment of the
203 roads. This type of anthropic influence must therefore be minimized ~~in order~~to generate
204 coherent flow direction (Li et al., 2013). Furthermore, the use of a breaching algorithm
205 allowed to generate hydrologically coherent DEMs prior to hydrographic modeling
206 (Lindsay, 2016b; Lindsay and Dhun, 2015). Physiographic factors must also be considered
207 during the modeling process as they significantly influence the location of channel heads
208 and the flow regime along streams. On the local scale, where the precipitation regime is
209 uniform (Tucker and Slingerland, 1996), slope, hydraulic force and sediment cohesion
210 generally dictates streambed formation (Dietrich and Dunne, 1978). The influence of these
211 factors is variable depending on the type of ~~surface~~Quaternary deposit (Dietrich and
212 Dunne, 1993; Dunne and Black, 1970; Montgomery and Dietrich, 1994).
213 ~~Surface~~Quaternary deposits can be used to assess which processes are involved in the
214 formation of a streambed. ~~Indeed, there~~There are two major types of ~~streambed~~ formation
215 processes. The first type involves surface processes, which occurs when soil that has low
216 permeability is exposed to rainfall amounts that exceed the infiltration capacity of the
217 ground, causing surface runoff (Horton, 1945). Then, when the power of the water exceeds
218 the cohesion of the sediments, usually in concavities, a streambed forms (Dietrich and

219 Dunne, 1978). The second type involves subsurface processes that occur when the
220 surfaceQuaternary deposits are thick and infiltrative. Water vertically infiltrates into the
221 ground and eventually reaches saturation at a junction with the water table, the bedrock, or
222 an inferior and less infiltrating deposit. Then, lateral movement of the groundwater occurs.
223 Water emerges from the ground when there is a change in slope or soil permeability.
224 Streambeds formed in this way tend to be heavily incised, with flow regimes that are more
225 stable than those formed through surface processes. Thus, the hydrological response of the
226 streams from subsurface processes is slightly affected by the intensity of rainfall (Dunne
227 and Black, 1970; Jensen et al., 2019; Wohl, 2018). Furthermore, it should be noted that
228 there is a gradient between these two processes for each stream. In order to properly detect
229 streambeds, it is essential to distinguish these processes through hydrological classification
230 according to surfaceQuaternary deposit type and land use.

231 SurfaceQuaternary deposit mapping has been standardized across the province, ~~including~~
232 ~~our study area. Information of Quebec and information~~ was collected through
233 photointerpretation conducted several years ago. Since photointerpretation was mainly
234 used to distinguish forest structures and land use, the true boundaries of the
235 surfaceQuaternary deposits are imprecise, in some cases. SurfaceQuaternary deposit
236 boundaries in agricultural areas are more accurate than those in forested areas because no
237 other information was mapped during the process. Regardless of these drawbacks,
238 standardized mapping provides a rough description of the nature and thickness of
239 surfaceQuaternary deposits.

240 Spatially heterogeneous surfaceQuaternary deposits in Quebec have been classified into
241 three categories and are described in Table 1 (Saucier et al., 1994). The purpose of this

242 classification step is to differentiate the two types of hydrological processes for headwater
 243 stream formation that were previously described (Dietrich and Dunne, 1993; Lessard,
 244 2020). These classifications consider the infiltration capacity and the water storage
 245 capacity of the ground (Dunne and Black, 1970). The two main variables considered were
 246 the potential thickness and the granulometry of the surfaceQuaternary deposits (Dietrich
 247 and Dunne, 1993; Wohl, 2018). Thus, the hydrological classes in Table 1 allow us to group
 248 together streams whose formation is driven by similar, and therefore theoretically
 249 homogeneous, hydrological processes.

251 **Table 1** : Hydrological classification according to surfaceQuaternary deposit types ~~and land~~
 252 ~~use~~

Hydrological class	<u>SurfaceQuaternary</u> deposits and land use -involved
Shallow soil	Glacial deposits without morphology such as till, frequent rock outcrops,
Thick soil with high infiltration rate (including anthropogenic land use)	Glacial deposits with morphology such as moraines, glaciofluvial deposits, fluvial deposits, coarse lacustrine and marine deposits, slope deposits and eolian deposits; <u>Anthropogenic Agricultural land use were, regardless of anthropic modifications due to linearization and deepening of streambeds, has been</u> included in this class

	(Treeless areas including agricultural fields, roads, urbanized areas and powerlines) as agriculture is mainly carried out on the above deposits.
Thick soil with low infiltration rate	Lacustrine and fine marine deposits, organic deposits.

253

254 The first analysis variable, called ‘D8’, refers to the D8 flow accumulation (O’Callaghan
 255 and Mark, 1984) produced with a 1 m resolution DEM. This variable was selected as it is
 256 the most common algorithm used to produce hydrographic networks. For meaningful
 257 correspondence analysis between this variable and field surveyed streams, the flow
 258 accumulation raster was aggregated at 3 m resolution according to the maximum value.
 259 Then, a maximum focal statistic of two pixels was applied. The purpose of this treatment
 260 was to ensure a 6 m analysis distance between the D8 and the edge of a real stream,
 261 represented in the database by a ~~geospatial~~vector line feature. This prevents the omission
 262 error from being overestimated.

263 The second analysis variable uses the D8 flow accumulation algorithm while considering
 264 flow direction error due to the elevation uncertainty of the LiDAR-derived DEM (Hengl et
 265 al., 2010; O’Callaghan and Mark, 1984). This variable, called ‘PROB’, quantifies the
 266 uncertainty associated with the position of the drainage network. This variable allows water
 267 diffusion processes to be simulated more adequately than the multiple flow direction
 268 algorithms that have been developed for this purpose (Freeman, 1991). Murphy et al.,
 269 (2009) noted a convergence of results between the single and multiple flow direction
 270 algorithms using high-resolution DEMs derived from LiDAR data. The use of a multiple

271 direction algorithm did not provide better results for simulating soil moisture. Indeed, the
272 dendritic flow pattern still appeared visible in the wetlands, even with the use of a multiple
273 flow direction algorithm, probably due to the microtopography present in these DEMs. The
274 elevation error in the DEM is directly related to the uncertainty of the LiDAR data
275 (Wechsler, 2007) and impacts the position of the hydrographic network (Lindsay, 2006).
276 This type of error is affected by the landform, and mainly occurs on gentle slopes and
277 slightly convex terrain (Hengl et al., 2010). Since this type of error is inherent to the shape
278 of the land, it is not affected by the size of the drainage area implied. The iterative method
279 described in Hengl et al. (2010) was reproduced in order to create the PROB variable. The
280 method is based on repeatedly computing a flow accumulation raster from an initial DEM
281 and several altered versions of the DEM. These altered versions are created by adding
282 random elevation errors to the initial DEM ~~in order~~ to reproduce the elevation errors from
283 the LiDAR data. The elevationAs describe by Richardson and Millard (2018) the typical
284 ground return elevations errors therefore had a standard deviation of 0.08 m, randomly
285 distributed over the DEM. A focal statistic of 3 m was used on the error raster to ensure
286 the spatial autocorrelation of errors. Based on the convergence observed by ~~(Lindsay;~~
287 (2006), 50 iterations were carried out. Then, each of the flow accumulation rasters were
288 thresholded to a 1.5 ha drainage area to sum the resulting binary stream network, where a
289 value of 1 indicated the presence of a streambed and a 0 indicated the absence of a
290 streambed. The matrix of the cumulative value was then normalized as a percentage to be
291 used as an analysis variable. This PROB variable revealed the extent of the diffusion
292 process of the water in hillsidesin valley bottoms, small wetland or riparian areas, where
293 the slope is relatively uniform-low or the topography slightly convex. The PROB variable

294 was produced with a 3-m resolution DEM from a 1 m resolution DEM that was aggregated
295 using the mean values. An average flow accumulation raster that corresponded to the
296 average of the 50 flow accumulations raster without thresholding was also produced. This
297 raster was used to create the analysis database and to calculate the drainage area of the
298 channel heads. To ensure a 6 m analysis distance as well as the D8 variable, a maximum
299 focal statistic of two cells was performed before summing or averaging the iterated
300 ~~raster~~rasters.

301 The third variable used for analysis is morphometric and allows for the complementary
302 detection of headwater streams (Lindsay, 2006; Tribe, 1992). The morphometric algorithm
303 used was the topographic position index, referred to as 'TPI'. This algorithm allowed for
304 the local detection of small incisions that might represent streambeds (Tribe, 1992). The
305 scale at which this variable is calculated strongly influences the morphometric feature that
306 is identified. When the scale is large, the variable will tend to identify valleys, while it
307 tends towards streambeds when the scale is small (Montgomery and Dietrich, 1992, 1994).
308 For the purposes of this paper, a relatively small scale of 6 to 30 m was used. This scale is
309 consistent with the width of the majority of inventoried streambeds. The DEM used to
310 calculate this variable had a resolution of 2 m and was derived from aggregating a 1 m
311 resolution DEM with the minimum values. The tool named 'Topographic Position Index'
312 in SAGA-GIS software was used to produce this variable (Guisan et al., 1999; Weiss,
313 2001). The TPI variable has not been normalized to ~~keep the homogeneity~~allow
314 comparison of the values between the different study areas.

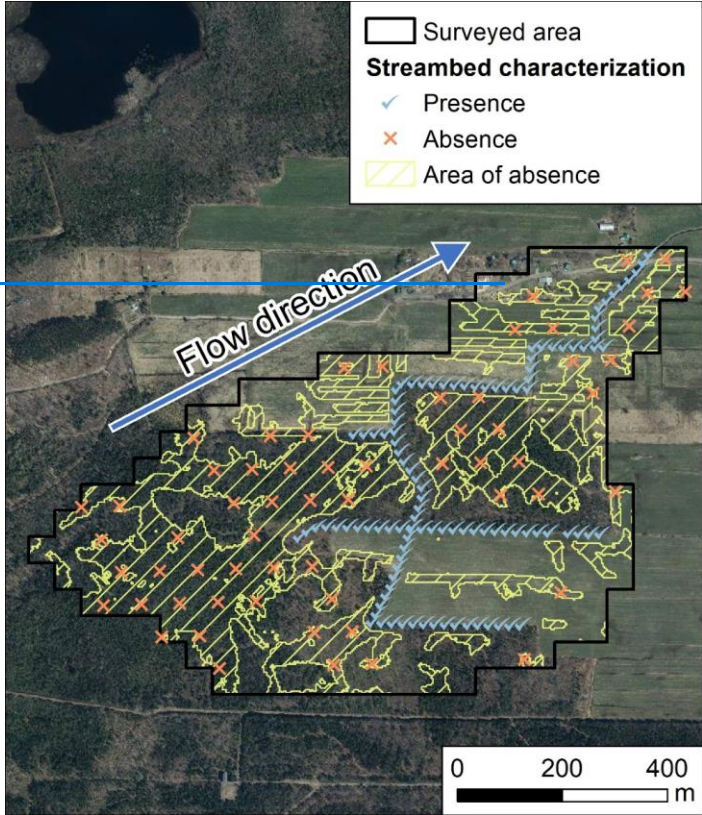
315 3.3. *Analysis database*

316 In order to perform the subsequent analyses, all actual streambeds were vectorized and geo-
317 interpreted according to the stream positions recorded in the field. It should be noted that
318 information on the flow regime was not used in this database. Instead, the presence of a
319 streambed was used to describe the presence or absence of a stream. Although some
320 ~~beds~~streambeds have been ~~excavated~~linearized and ~~channelized~~deepened, particularly in
321 ~~anthropogenic~~anthropic lands, a ~~bed~~streambed was considered to be present only when
322 natural fluvial processes allow it to be maintained. ~~The geospatial~~The presence of geo-
323 ~~interpreted vector~~ lines ~~indicating~~features indicated the exact location of the streambeds
324 ~~and~~ were complemented by a 50 m x 50 m grid to represent the complete surveyed area.
325 Thus, areas without a ~~geospatial~~vector line feature have been assumed ~~to~~as not
326 ~~contain~~containing streambeds.

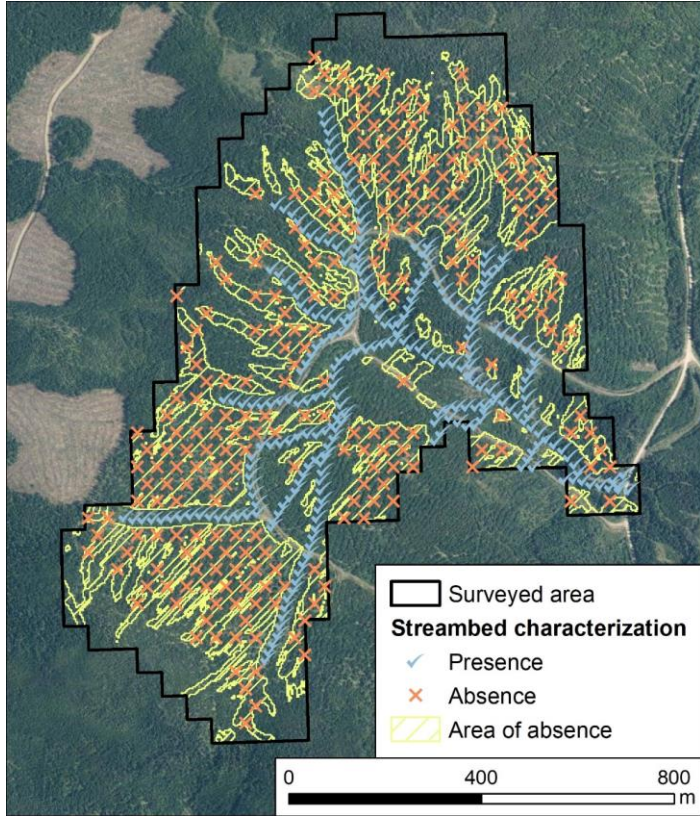
327 Positions representing the presence of ~~streams~~streambeds were systematically located
328 every 20 m along ~~geospatial~~vector lines features that described real streams. Then,
329 positions representing the absence of a streambed were located according to a sampling
330 principle based on minimum flow accumulation where it was still ~~possible~~coherent to
331 observe the presence of a ~~stream~~streambed. First, within the grid of the surveyed area, the
332 average flow accumulation raster was thresholded at 0.11 ha. This threshold represents the
333 lowest drainage area for initiation of a channel head according to (Lessard, (2020). Then,
334 the resulting raster was converted to a polygon. Following that step, a 20 m buffer zone
335 was removed around the ~~geospatial~~vector lines features that represent real streams. ~~Finally,~~
336 ~~absence positions were systematically located according to a hexagonal distribution in the~~
337 ~~final resulting polygon.~~ Thus, polygons identifying absence positions were located only in
338 areas with a minimum ~~1400 m²~~of 0.11 ha mean drainage area and a minimum distance of

339 20 m from any real streams. Finally, absence positions were systematically located
340 according to a hexagonal distribution in the final resulting polygon. The number of absence
341 positions was equalized with the number of presence positions for each natural region
342 within the Quebec ecological reference framework.

343 The analysis database was therefore composed of positions describing both the presence
344 and the absence of streambeds (Fig. 2). The values for the three variables described in the
345 previous section (D8, PROB and TPI) were extracted for all presence and absence
346 positions.



347



349 **Figure 2** : Analysis database of positions indicating the presence and absence of
 350 streambeds (Aerial images from continuous imagery of the Government of Quebec;
 351 MRNF). [Color is not required for this figure. Single column fitting figure.]

352

353 *3.4. Statistical analysis*

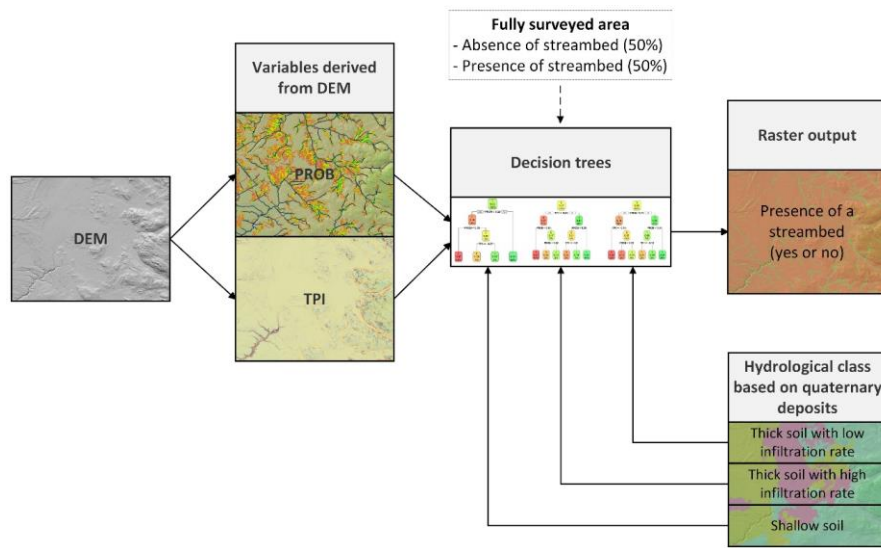
354 A total of nine logistic regression models were produced, one for each explanatory variable
 355 and hydrologic class combination. Response variable was the presence (1) or the absence
 356 (0) of a streambed. The area under the ROC (Receiver Operating Characteristic) curve was
 357 used to evaluate model performance (Fawcett, 2006). The ROC curve plots the true positive

358 rate (1 minus omission) relative to the false positive rate (commission). This curve shows
359 the performance of a given variable by determining the Area Under the Curve (AUC) and
360 how the increase in the true positive rate will lead to an increase in the false positive rate.
361 A model with a high AUC will provide a better balance between these two measurements
362 and will produce better results. Thus, the AUC provides a measure of the ability of the
363 individual variables to detect a streambed.

364 Next, four streambed models were compared to each other. Detection performance was
365 calculated according to hydrological class and using Cohen's kappa, which is a measure of
366 agreement between the true positive rate and the false positive rate (Cohen, 1960).

367 The first model examined was the GRHQ. An analysis distance of 6 m was used ~~in order~~
368 to compare properly the performance of the GRHQ with the other models. Two of the other
369 three models corresponded to two different thresholds that were applied to the D8 variable,
370 which is one of the most commonly used variables for generating stream networks. The
371 first threshold was the median of the average drainage area of the channel heads surveyed
372 in the field (referred to as Channel head; [Fig. 3](#)). The second threshold was the one that
373 maximized Cohen's kappa for the variable D8 (referred to as Max Kappa). The last model
374 that was compared is based on a supervised classification approach. This approach groups
375 observations according to explanatory variables based on previously determined groups,
376 also known as the response variable. In this case, the response variable was the presence
377 or absence of a streambed. Classification And Regression Tree (CART) approach was used
378 because ~~it is simple to apply~~ of its ease of understanding the results and applying them over
379 a large territorywide area (Breiman et al., 1984). ~~This model was called CART.~~ One tree
380 was produced for each hydrologic class in order to describe the formation of headwater

381 streams from homogeneous hydrologic processes. ~~Based on the literature, different~~
382 ~~variables were used for each hydrological class. The PROB variable was the only one that~~
383 ~~was used to detect streambeds in shallow soil, as the bedrock is usually close to the surface~~
384 ~~of the ground and not very suitable for incisions (Jensen et al., 2018). For the other two~~
385 ~~hydrological classes in thick soils, the TPI and PROB variables were used. The surface~~
386 ~~deposits in these classes are not consolidated, allowing the ground to be incised. This can~~
387 ~~then be detected by different morphometric indices (Montgomery and Dietrich, 1994). The~~
388 ~~depth and number of branches in the classification trees have been limited in order to~~
389 ~~prevent overfitting (Fürnkranz, 1997).~~
390 The TPI and PROB variables were used for each hydrological class to produce trees. A
391 flow chart of the general method is shown in Figure 3. The depth and number of branches
392 in the classification trees have been pruned in order to prevent overfitting and it was
393 therefore not necessary to split the data into a training and a testing set (Fürnkranz, 1997).



394

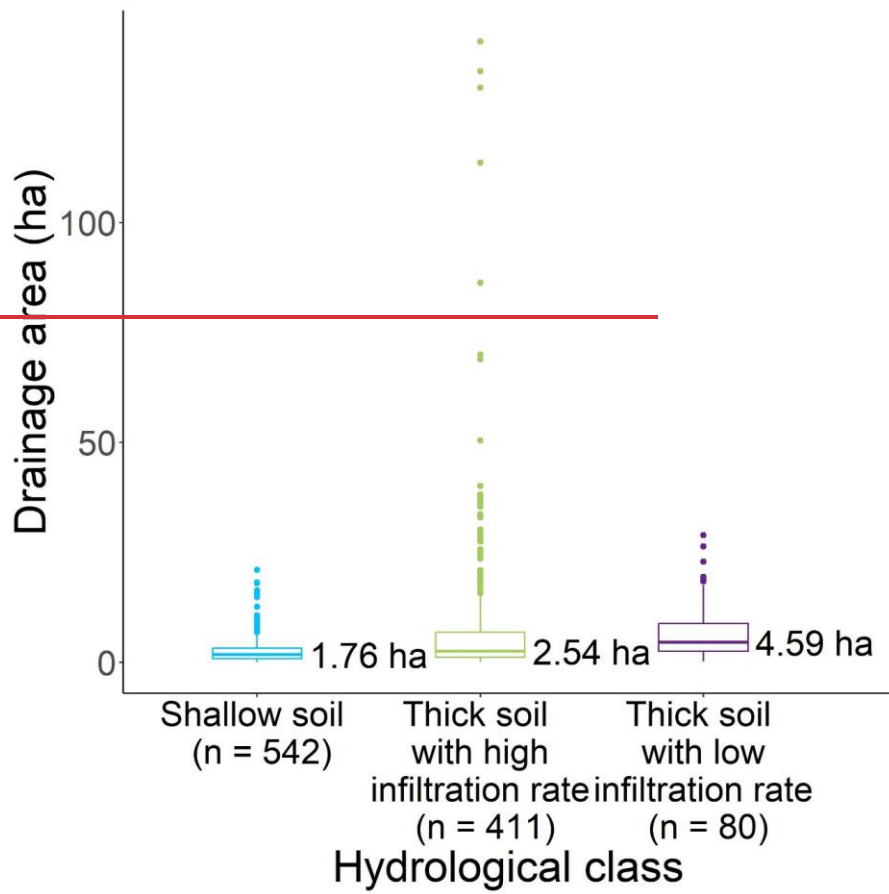
395 Figure 3 : Flowchart showing the methodology used to produce a raster describing the
396 presence of a streambed using classification trees [Color is not required for this figure.
397 2 column fitting figure.]

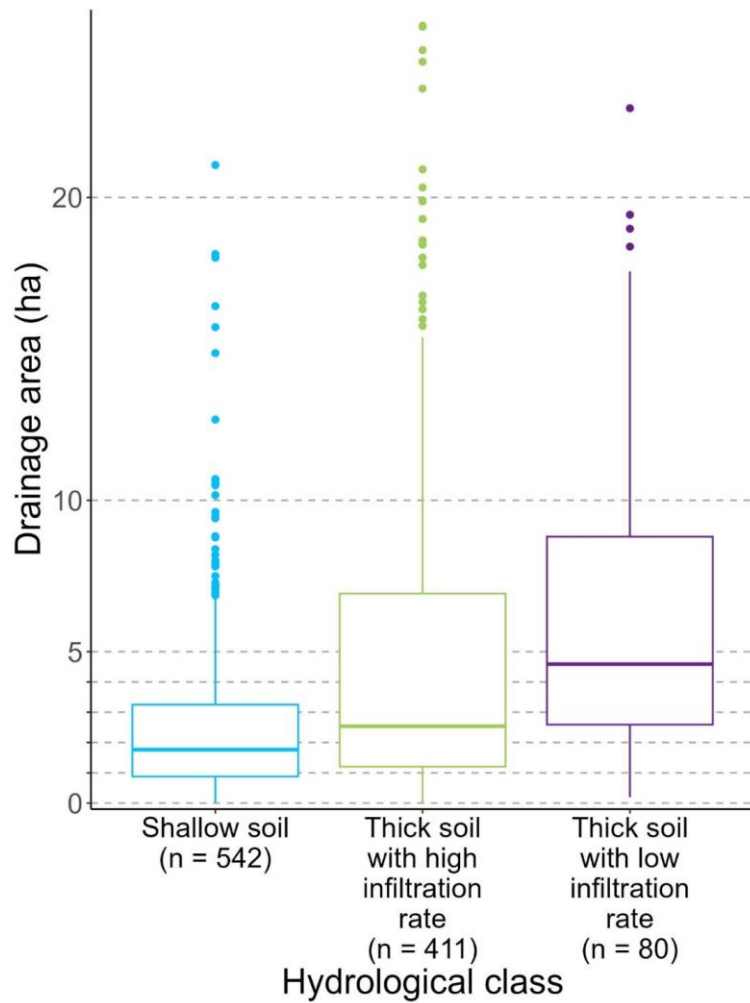
398

399 4. Results

400 A total of 464.7 km of streams were surveyed over ~~a known territory~~an area of 161.5 km².
401 The positions ~~for 1033~~of 1 033 channel heads indicating the beginnings of streambeds were
402 determined. The average drainage areas of the channel ~~head~~heads are presented in Fig. ~~34~~
403 using whisker boxes according to hydrological class. Figure ~~34~~ shows that for shallow soil,
404 the average drainage area is less variable than for thick soils. For thick ~~soil~~soil with low
405 infiltration ~~rates~~rate, the average drainage area tends to be higher. Slope-drainage area
406 curves and a visualization of different streambeds for each hydrological class are presented
407 in Supplementary Materials.

408





410

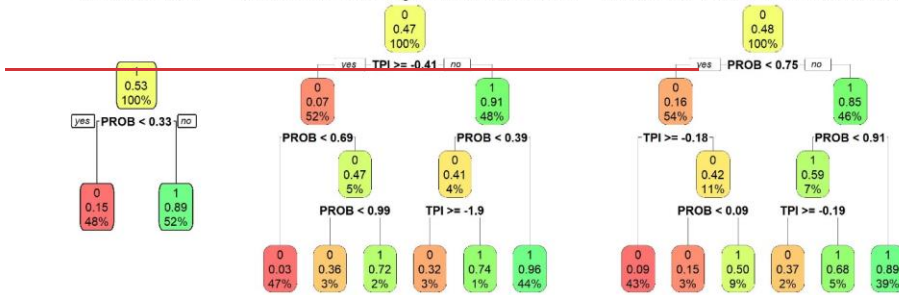
411 **Figure 34** : Distribution of mean drainage areas of channel heads according to hydrological
 412 class. Median values are shown. [Color is not required for this figure. Single column
 413 fitting figure.]

414

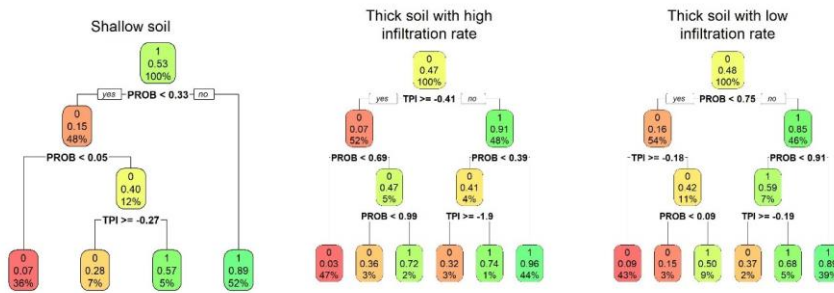
415 The analysis database contains a total of 40 354 positions describing streambeds (20 177

416 with streambeds present and 20 177 with streambeds absent) ~~located in the entire surveyed~~
417 ~~area~~). A correlation matrix between the analysis variables showed that PROB is negatively
418 correlated with TPI, with an R of -0.57. This variable therefore identifies where the water
419 converges, which usually corresponds with the locations of incisions. The ~~other variables~~
420 ~~were~~ D8 variable was not correlated with ~~each~~ other ones.
421 ~~Three~~ The classification trees according to hydrological class are presented in Fig. 45. The
422 tree for shallow soil shows that when PROB exceeds a threshold of 0.33, a streambed is
423 generally present. At the left side of the tree, when the PROB is very low, below 0.05, the
424 streambed is generally absent. Otherwise, the TPI indicates whether a streambed is present
425 or absent. For thick soil with a high infiltration rate, the incision indicated by the TPI first
426 explains the presence of a streambed. When the incision is greater or equal to -0.41,
427 indicating a small incision, PROB must be very high ~~in order~~ to indicate the presence of a
428 streambed, at 0.99. When there is a larger incision, a lower value for PROB can identify
429 the presence of a streambed. Thus, when the ground is relatively well incised with a TPI
430 value smaller than -0.41, PROB only needs to be higher than 0.39 to detect a streambed.
431 In thick soil with a low infiltration rate, PROB provides the initial information regarding
432 the presence or absence of a streambed. Depending on the different PROB thresholds, TPI
433 then determines the presence or absence of a streambed.
434

Shallow soil Thick soil with high infiltration rate Thick soil with low infiltration rate



435



436

437 **Figure 45** : Classification trees to detect the presence of streambeds according to variables
 438 D8, PROB and TPI and hydrological class. The colors red, orange, yellow and green
 439 represent very low, low, medium, and high probability respectively. [Color is not required
 440 for this figure. 2 column fitting figure.]

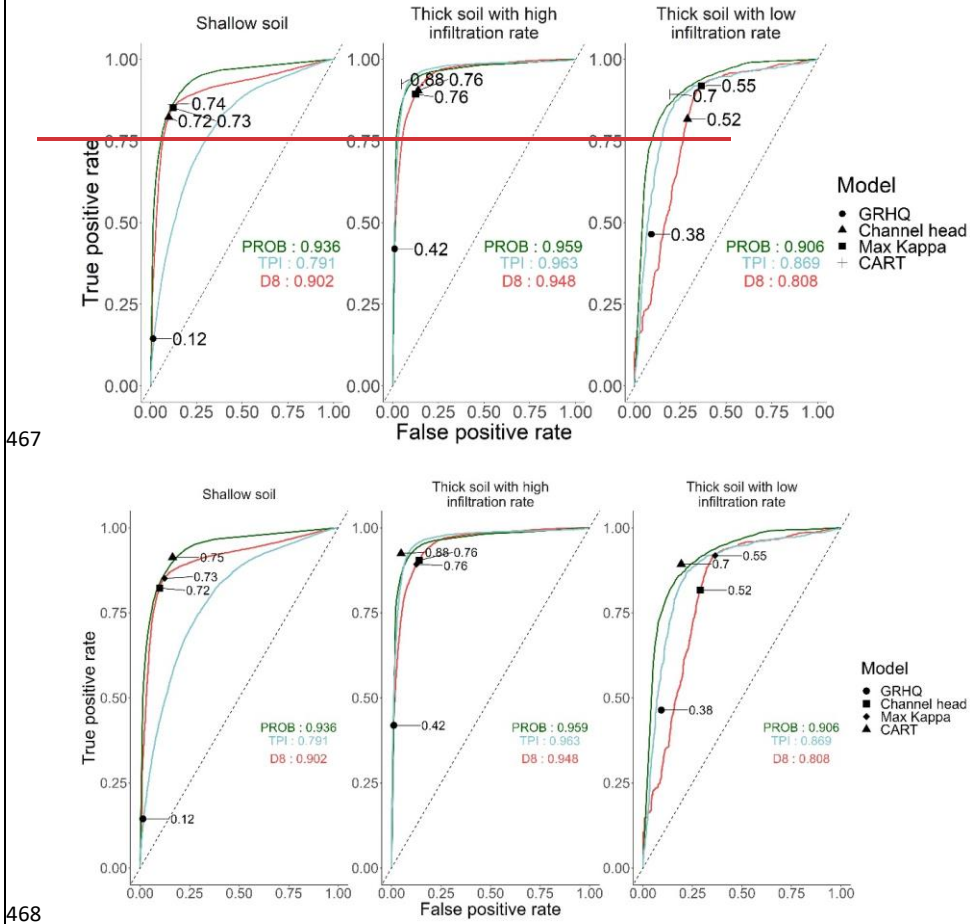
441

442 Figure 56 compares the AUC of individual variables, thus their potential to detect a
 443 streambed. The performance of the four streambed models is also presented. This figure
 444 shows that for the three hydrological classes, PROB performs more effectively than D8

a mis en forme : Police :Non Gras

445 when it comes to detecting streambeds. For thick soil classes, the incision variable TPI has
446 a higher AUC than D8. For shallow soil, the opposite is true. Compared to the other models,
447 the GRHQ has a very low true positive rate, meaning it omits many streams regardless of
448 the hydrologic class. However, the performance of GRHQ is higher for thick ~~soils~~soil than
449 for shallow ~~soils~~soil. For shallow ~~soils~~soil, although the false positive rate is slightly lower
450 for D8 thresholded with channel heads (Channel head), the Cohen's kappa of the
451 classification tree (CART) is still higher. The performance of the maximum Kappa of D8
452 (Max Kappa) is still very similar to the one of the classification tree (CART). ~~Figure 5 also~~
453 ~~shows that the performance of the classification tree (CART) for shallow soil is not in the~~
454 ~~upper left part of the ROC curve of the variable PROB. This observation is consistent with~~
455 ~~the fact that only this variable was used to calibrate this model. Nevertheless, for both thick~~
456 ~~soil classes~~Figure 6 also shows that for each class, the performance of the classification
457 trees (CART) is in the upper left part of the ROC curve of the ~~variable PROB~~variables
458 ~~used alone~~. This means that the ~~addition~~combination of the incision variable TPI ~~with the~~
459 ~~PROB variable~~ improves the detection of streambeds. For thick ~~soils~~soil with high
460 infiltration ~~rates~~rate, the two thresholding methods (Channel head and Max Kappa) yielded
461 similar performances, although they did not perform as well as the classification tree
462 (CART). The performance of the classification tree (CART) is also higher than both D8
463 thresholding methods for thick ~~soils~~soil with low infiltration ~~rates~~rate. However, the
464 method using the maximum Kappa (Max Kappa) yields a higher rate of true positives than
465 the thresholding method using the channel heads (Channel head).

466



467

468

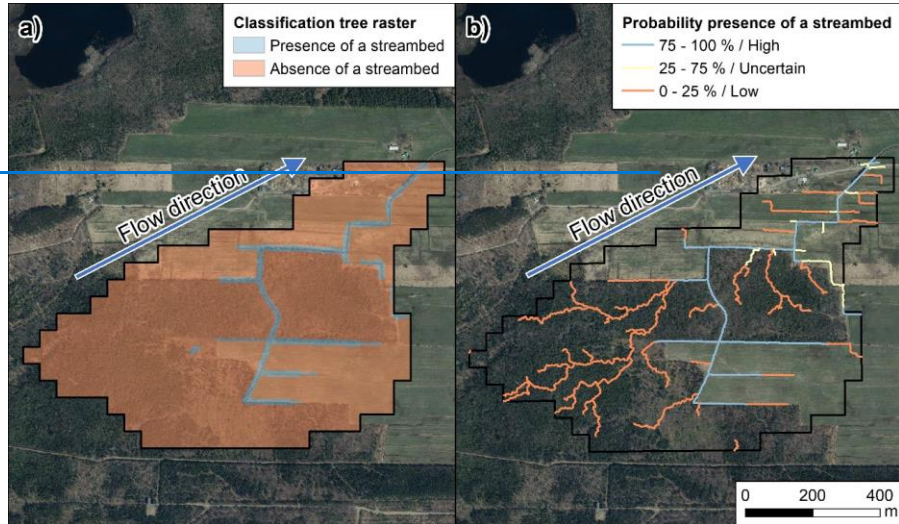
469 **Figure 56** : ROC curve and AUC values from the logistic regressions of the three variables
 470 according to hydrological class. The performance of the streambed models using Cohen's
 471 kappa is also presented. [Figure 5 about here. [Color is not required for this figure. 2
 472 column fitting figure.]

473

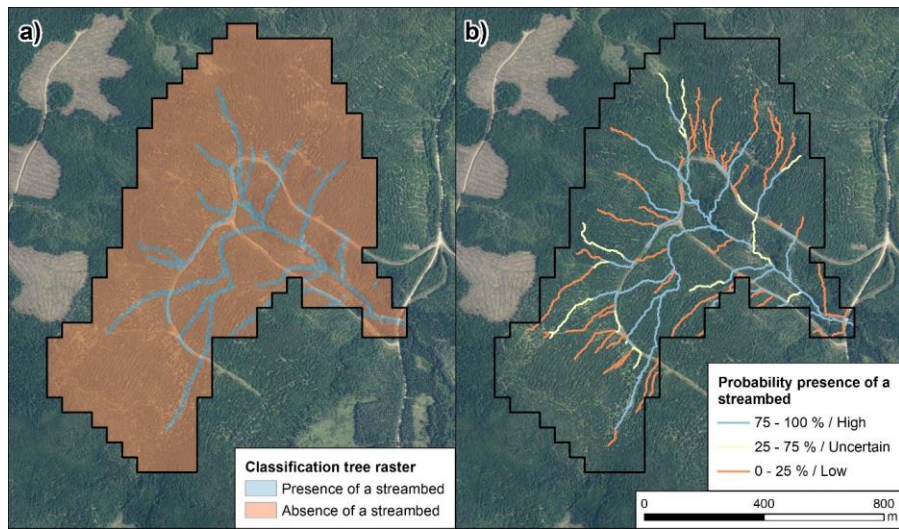
474 **5. Discussion**

475 The results suggest that the classification tree (CART) can detect streambeds more
476 accurately than the other methods tested. By integrating different topographic indices and
477 ground information such as ~~surface~~Quaternary deposits, the detection of headwater
478 streambeds is much more efficient in large watersheds, despite ~~the high~~ anthropization of
479 the ground as agricultural fields that ~~is~~are sometimes present. In addition, as the results of
480 the classification trees are rasters (Fig. ~~6-a~~);7a), they can be easily integrated within
481 attribute table of a drainage network by calculating the mean using a zonal statistic to assess
482 the probability presence of a streambed (Fig. ~~6-b~~);7b). This integration can be done without
483 altering the course or thresholds of the hydrographic network. Each segment can therefore
484 be truncated according to the presence or absence of the stream predicted by the model.
485

486



487



488

489 **Figure 67** : Classification tree that has been integrated into the segments of a hydrographic
490 network to assess the probability presence of a streambed (b) (Aerial images from
491 continuous imagery of the Government of Quebec; MRNF). [Color is not required for

492 **this figure. 1.5 column fitting figure.]**

493

494 The classification tree (CART) drastically increases the true positive rate compared to the
495 GRHQ. This is because the GRHQ was based on aerial photographs that were primarily
496 used to characterize vegetation and forest structure. Photointerpretation of these images
497 did not allow for the detection of streambeds formed by local fluvial processes under the
498 forest cover (Lessard, 2020). At most, photointerpretation enables the identification of
499 valleys, for example, on thick ~~soils~~soil (Montgomery and Dietrich, 1994). For this reason,
500 the GRHQ omits fewer streams in thick soil than in shallow soil.

501 The PROB variable improved the detection of streambeds compared to the conventional
502 use of only the D8 variable, since it has been thresholded to accurately match the lowest
503 drainage areas of the channel heads. According to Fig. 34, the 1.5 ha threshold accounts
504 for ~~the majority~~most of the channel heads. However, the drainage areas of the channel
505 heads are generally higher for thick ~~soils~~soil with low infiltration ~~rates~~. ~~The majority~~rate
506 ~~and could therefore lead to higher false positive rate~~. Most of the surveyed streams in this
507 hydrologic class are located in the Abitibi Lowlands natural province. ~~Some~~Furthermore,
508 ~~it is important to note that some~~ of the drainage areas of the channel heads in shallow soil
509 are smaller than 1.5 ha.

510 For the shallow soil hydrological class, the PROB variable improves streambed detection
511 only when a false positive rate of at least 0.12 is specified. Figure 56 shows that for a false
512 positive rate of 0.25, for example, PROB has a higher true positive rate than the D8
513 variable. Streambeds that were not omitted with a PROB threshold greater than 0.12 were
514 mostly small streams with highly variable positions due to the slightly upstream convex

515 topography (Hengl et al., 2010). It seems that these streambed presence positions have very
516 low PROB values (48% of these positions have a probability below the 0.33 threshold used;
517 Fig. 45). The 0.33 PROB threshold enabled a false positive rate that is much lower than
518 0.25. In fact, the false positive rate was only 0.12. With this 0.33 threshold, the performance
519 of PROB was almost identical to D8. ~~This is indicated on the figure by the two ROC curves~~
520 ~~that were at their closest to each other at approximately the same place as the classification~~
521 ~~tree model (CART) (Fig. 5). In order to (Fig. 6). To~~ increase the true positive rate while
522 using the PROB variable, the threshold could be decreased to allow the smallest streams to
523 be identified. However, this modification would increase the false positive rate.

524 The poor performance of the TPI variable for shallow soil is due to the fact that the
525 ~~surface~~Quaternary deposits are generally thin and the slopes are frequently steep. The
526 ground is therefore less prone to erosion and incision than for the other two hydrological
527 classes (Jensen et al., 2018; Montgomery and Dietrich, 1994). Indeed, the parameters used
528 to compute TPI do not enable the detection of small streambeds if they are not located in a
529 valley or in a larger incision. Furthermore, the hydrological processes involved in this class
530 are mostly surface flow and not subsurface flow. It is for this reason that D8 and PROB,
531 which tend to be able to ~~quite precisely~~recreate surface flow quite precisely, are the best
532 performing variables in this hydrological class (Julian et al., 2012; Wohl, 2018).

533 The incision variable TPI performed better in thick ~~soil~~soil with high infiltration ~~rates~~rate.
534 This seems to be due to the fact that unlike shallow ~~soil~~soil which are generally thin,
535 infiltrative ~~soil~~soil are thick and unconsolidated. Thus, the main hydrological process for
536 this hydrological class is a subsurface process, where the water table plays an important
537 role in the initiation of streambeds. Water infiltrates vertically into the permeable ~~surface~~

538 ~~deposits~~deposit and recharges the groundwater (Dunne and Black, 1970). The locations of
539 the channel heads do not correspond to specific drainage areas that can be identified by
540 flow accumulation variables, but rather to local incisions formed by gully processes
541 where groundwater intersects the ground surface (Dietrich and Dunne, 1993; Wohl, 2018).
542 This process occurs where there is a significant change in slope or soil permeability. The
543 emergence of water from the ground leads to progressive gully processes that can be detected by
544 incision variables (Montgomery and Dietrich, 1994). In this context, groundwater depth
545 variables such as depth-to-water (DTW; (White et al., 2012)) could be used to explain the
546 presence of streams in areas where a water table is present. It is important to mention that
547 the DTW is very sensitive to parameterization and more research is needed for its proper
548 use (Drolet, 2020).

549 Streambeds were better detected using solely PROB instead of D8 for thick ~~soil~~soil with
550 low infiltration ~~rate~~rate, which occur in territories where there is a high proportion of
551 wetlands and gentle slopes. The PROB variable mostly reduces the number of commission
552 cases. For example, in Fig. 56, PROB had a much lower false positive rate than D8 for the
553 same true positive rate of 0.75. This large reduction in the false positive rate achieved with
554 PROB reflects the ability of this variable to reproduce a diffuse flow on very flat or slightly
555 convex terrains (Hengl et al., 2010). Indeed, in 78 % of cases, the positions that correspond
556 to an absence of a streambed and that are corrected with PROB are wetlands. This is
557 noteworthy because wetlands represent only 64 % of these positions in this hydrological
558 class. Thus, the PROB variable, using uncertain DEM elevation information, can recreate
559 more realistic behavior of the water, especially in thick ~~soil~~soil with low infiltration
560 ~~rate~~rate. By using both PROB and TPI variables (Fig. 45), streambed detection for this

561 hydrological class can be improved compared to the use of a single variable. Because the
562 deposits are unconsolidated and the ground can be incised (Dietrich and Dunne, 1993), the
563 classification tree is in the upper left part of the ROC curve for the PROB variable as well
564 as for the hydrological class with the high infiltration. The use of the TPI variable therefore
565 provides an advantage.

566 A limitation of the classification tree method is that the surfaceQuaternary deposit mapping
567 is not accurate enough for all local hydrological issues. A visual inspection revealed some
568 inconsistencies in the surfaceQuaternary deposit mapping within the same hydrological
569 class.

570 Another limitation is associated with the anthropization and linearization of natural
571 streams. While a streambed is the result of a natural fluvial formation process that leads to
572 ground erosion, an anthropogenicanthropic ditch is an artificial bed that is formed by
573 mechanized digging. However, it is common for naturally formed streambeds to have been
574 excavated and linearized in agricultural areas. In these cases, it becomes very difficult to
575 distinguish a streambed from an anthropogenicanthropic ditch, even in the field.
576 Excavation concentrates the flow of water in the artificial bed (Moussa et al., 2002). Thus,
577 an area with previously no water flow could now be considered a streamstreambed
578 (Roelens et al., 2018). Automated detection methods are therefore likely to be much less
579 reliable in these situations.

580 We believe that the method described for calibrating the classification tree model is simple
581 and robust enough to be applied in a different climatic and geomorphiegeomorphologic
582 context with local data describing headwater streambeds. An accurate LiDAR derived

583 headwater streambed mapping is a powerful tool for government and local organizations
584 involved in water management and protection.

585

586 **6. Conclusion**

587 The classification tree method presented in this paper has improved the detection of
588 headwater streambeds for different hydrological ~~contexts~~ processes over large watersheds.

589 Reliable and consistent results were obtained by developing a comprehensive field
590 database. The variable PROB, which describes the probability of occurrence of a
591 streambed, was used to correct errors associated with the positioning of streambeds. This
592 variable allowed for marginal corrections of streambeds in shallow soil, particularly when
593 a high threshold was used. In order to more precisely explain where streams initiate in
594 shallow soil, variables characterizing the composition of the upstream watershed such as
595 the average upstream slope or the composition of deposits should be explored. The variable
596 TPI, which characterized small-scale incisions, significantly improved the detection of
597 streambeds in both thick soil hydrological classes when combined with the PROB variable.

598 The small-scale incision variable worked better in ~~soils~~ soil with high infiltration ~~rates~~ rate
599 and the probability of occurrence worked better in ~~soils~~ soil with low infiltration ~~rates~~ rate.

600 The increased complexity of the methods (inputs and parameterization) makes the
601 optimizations more difficult for ~~very~~ large and complex territories. ~~It is difficult to integrate~~
602 ~~the influence of-~~ The integration of all physiographic variables into a single model ~~and~~
603 ~~improvements require~~ requires multiple iterations which leads to high complexity. ~~The~~
604 ~~integration of case~~ Case studies could improve models by directly focusing on some of the
605 identified limitations. It is also important to consider that the input data may sometimes be

606 unreliable, such as those for the road network, culverts, ~~surface~~Quaternary deposits, and
607 land use. Thus, ~~future~~ developments, such as those integrating ~~surface~~Quaternary deposits,
608 will ~~not~~hardly be ~~improve~~possible if the quality of the raw data remains unchanged. Visual
609 interpretation of map products and verification by an expert with a good knowledge of the
610 area is an essential step that should not be neglected under any circumstances.

611

612 **Author contribution**

613 Francis Lessard and Naïm Perreault contributed to the research project by providing
614 expertise in methodology, software development, formal analysis, investigation, data
615 curation, writing, and visualization. Their contributions encompassed various stages, from
616 data collection and analysis to manuscript preparation.

617

618 Sylvain Jutras supervised the project, provided conceptual guidance, and played a role in
619 writing and reviewing the manuscript. Additionally, Jutras secured funding for the project
620 and managed administrative tasks related to its execution.

621

622 **Competing interest**

623 The authors declare that they have no conflict of interest.

624

625 **Acknowledgements**

626 The authors thank Quebec's Ministère de l'Environnement et de la Lutte contre les
627 changements climatiques (MELCC) and Ministère des Forêts, de la Faune et des Parcs
628 (MFFP), which funded this research project. This project would not have been possible

629 without the exceptional collaboration of the MELCC's and MFFP's LiDAR mapping
630 team, together with the many students and research associates who contributed to the
631 numerous field surveys.

632

633 **Data Availability**

634 Data and code can be found at https://github.com/FraLessard/headwater_streambeds.git,
635 hosted at GitHub (Lessard and Perreault, ~~2022~~2023).

636

637 **References**

638 Alexander, R. B., Boyer, E. W., Smith, R. A., Schwarz, G. E., Moore, R. B.: The role of
639 headwater streams in downstream water quality. *Journal of the American Water*
640 *Resources Association*, 43(1), 41–59. [https://doi.org/10.1111/j.1752-](https://doi.org/10.1111/j.1752-1688.2007.00005.x)
641 [1688.2007.00005.x](https://doi.org/10.1111/j.1752-1688.2007.00005.x), 2007.

642 Band, L. E.: Topographic Partition of Watersheds with Digital Elevation Models. *Water*
643 *Resources Research*, 22(1), 15–24. <https://doi.org/10.1029/WR022i001p00015>,
644 1986.

645 Blouin, J., and Berger, J.-P. : Guide de reconnaissance des types écologiques de la région
646 écologique 5a – Plaine de l’Abitibi. Ministère des Ressources naturelles du Québec,
647 Forêt Québec, Direction des inventaires forestiers, Division de la classification
648 écologique et productivité des stations. 180 pp., 2002.

649 Blouin, J., and Berger, J.-P. : Guide de reconnaissance des types écologiques des régions
650 écologiques 5e – Massif du lac Jacques-Cartier et 5f – Massif du mont Valin.
651 Ministère des Ressources naturelles, de la Faune et des Parcs, Forêt Québec,

Code de champ modifié

652 Direction des inventaires forestiers, Division de la classification écologique et
653 productivité des stations. 194 pp., 2004.

654 Breiman, L., Friedman, J. H., Olshen, R. A., & Stone, C. J.: Classification And Regression
655 Trees. Routledge. <https://doi.org/10.1201/9781315139470>, 1984.

Code de champ modifié

656 Cho, H. C., Clint Slatton, K., Cheung, S., & Hwang, S.: Stream detection for LiDAR digital
657 elevation models from a forested area. International Journal of Remote Sensing,
658 32(16), 4695–4721. <https://doi.org/10.1080/01431161.2010.484822>, 2011.

Code de champ modifié

659 Cohen, J.: A Coefficient of Agreement for Nominal Scales. Educational and Psychological
660 Measurement, 20(1), 37–46. <https://doi.org/10.1177/001316446002000104>, 1960.

Code de champ modifié

661 Conrad, O., Bechtel, B., Bock, M., Dietrich, H., Fischer, E., Gerlitz, L., Wehberg, J.,
662 Wichmann, V., & Böhner, J.: System for Automated Geoscientific Analyses
663 (SAGA) v. 2.1.4. Geoscientific Model Development, 8(7), 1991–2007.
664 <https://doi.org/10.5194/gmd-8-1991-2015>, 2015.

Code de champ modifié

665 [Couture, T.: Fish biodiversity and morphological quality in small agricultural streams of
666 Montérégie, Québec. Master thesis, Department of Geography, Planning and
667 Environment. Concordia University. 75 pp., 2023.](#)

a mis en forme : Anglais (Canada)

668 Creed, I. F., Lane, C. R., Serran, J. N., Alexander, L. C., Basu, N. B., Calhoun, A. J. K.,
669 Christensen, J. R., Cohen, M. J., Craft, C., D'Amico, E., De Keyser, E., Fowler, L.,
670 Golden, H. E., Jawitz, J. W., Kalla, P., Katherine Kirkman, L., Lang, M. W.,
671 Leibowitz, S. G., Lewis, D. B., Marton, J., McLaughlin, D. L., Raanan-Kiperwas
672 H., Rains M. C., Rains K. C., Smith, L.: Enhancing protection for vulnerable
673 waters. Nature Geoscience, 10(11), 809–815. <https://doi.org/10.1038/NGEO3041>,
674 2017.

Code de champ modifié

675 Dietrich, W. E., and Dunne, T.: Sediment budget for a small catchment in mountainous
676 terrain. *Z. Geomorph. N. F., Suppl. Bd.*, 29, 191–206., 1978.

677 Dietrich, W. E., and Dunne, T.: The Channel head. In: Beven K. and Kirkby M.J., Eds.,
678 Channel Network Hydrology, Wiley, New York, 175-219., 1993.

679 Direction de l'expertise en biodiversité: Guide d'utilisation du Cadre écologique de
680 référence du Québec (CERQ). Ministère du Développement durable, de
681 l'Environnement et de la Lutte contre les changements climatiques (MDDELCC),
682 Québec. 24 pp., 2018.

683 Drolet, E. : Identification des zones de contrainte de drainage aux opérations forestières à
684 l'aide des données lidar. Master thesis. Department of Wood and Forest Science.
685 Université Laval. 62 pp., 2020.

686 Dunne, T., and Black, R. D.: An Experimental Investigation Runoff Production in
687 Permeable Soils. *Water Resources Research*, 6(2), 478–490.
688 <https://doi.org/10.1029/WR006i002p00478>, 1970.

689 Elmore, A. J., Julian, J. P., Guinn, S. M., & Fitzpatrick, M. C.: Potential Stream Density in
690 Mid-Atlantic U.S. Watersheds. *PLoS ONE*, 8(8), e74819.
691 <https://doi.org/10.1371/journal.pone.0074819>, 2013.

692 Estrada, D.: Smart Device / GNSS Receiver Assessment Study for Hydrographic. Office
693 of the State Engineer Information Technology Services Bureau GIS (OSE GIS). 48
694 pp., 2017.

695 Fairfield, J., and Leymarie, P.: Drainage Networks From Grid Digital Elevation Models.
696 *Water Resources Research*, 27(5), 709-717. <https://doi.org/10.1029/90WR02658>,
697 1991.

Code de champ modifié

Code de champ modifié

Code de champ modifié

698 Fawcett, T.: An introduction to ROC analysis. *Pattern Recognition Letters*, 27(8), 861–
699 874. <https://doi.org/10.1016/j.patrec.2005.10.010>, 2006.

Code de champ modifié

700 Freeman, M. C., Pringle, C. M., & Jackson, C. R.: Hydrologic connectivity and the
701 contribution of stream headwaters to ecological integrity at regional scales. *Journal*
702 *of the American Water Resources Association*, 43(1), 5–14.
703 <https://doi.org/10.1111/j.1752-1688.2007.00002.x>, 2007.

Code de champ modifié

704 Freeman, T. G.: Calculating catchment area with divergent flow based on a regular grid.
705 *Computers and Geosciences*, 17(3), 413–422. [https://doi.org/10.1016/0098-](https://doi.org/10.1016/0098-3004(91)90048-I)
706 [3004\(91\)90048-I](https://doi.org/10.1016/0098-3004(91)90048-I), 1991.

707 Fürnkranz, J.: Pruning Algorithms for Rule Learning. *Machine Learning*, 27, 139–172.
708 <https://doi.org/10.1023/A:1007329424533>, 1997.

Code de champ modifié

709 Gosselin, J.: Guide de reconnaissance des types écologiques des régions écologiques 3a –
710 Collines de l’Outaouais et du Témiscamingue et 3b – Collines du lac Nominique.
711 Ministère des Ressources naturelles du Québec, Forêt Québec, Direction des
712 inventaires forestiers, Division de la classification écologique et de la productivité
713 des stations. 188 pp., 2002.

714 Gosselin, J.: Guide de reconnaissance des types écologiques de la région écologique 3d -
715 Coteaux des basses Appalaches. Ministère des Ressources naturelles et de la Faune,
716 Direction des inventaires forestiers, Division de la classification écologique et
717 productivité des stations. 186 pp., 2005a.

718 Gosselin, J.: Guides de reconnaissance des types écologiques de la région écologique 2b -
719 Plaine du Saint-Laurent. Ministère des Ressources naturelles et de la Faune,
720 Direction des inventaires forestiers, Division de la classification écologique et

721 productivité des stations. 188 pp., 2005b.

722 Goulden, T., Hopkinson, C., Jamieson, R., and Sterling, S.: Sensitivity of watershed
723 attributes to spatial resolution and interpolation method of LiDAR DEMs in three
724 distinct landscapes. *Water Resources Research*, 50(3), 1908-1927.
725 <https://doi.org/10.1002/2013WR013846>, 2014.

726 Guisan, A., Weiss, S. B., and Weiss, A. D.: GLM versus CCA spatial modeling of plant
727 species distribution. *Plant Ecology*, 143(1), 107–122.
728 <https://doi.org/10.1023/A:1009841519580>, 1999.

729 Hafen, K. C., Blasch, K. W., Rea, A., Sando, R. and Gessler, P. E. : The Influence of
730 Climate Variability on the Accuracy of NHD Perennial and Nonperennial Stream
731 Classifications. *Journal of the American Water Resources Association*, 56(5), 903-
732 916. <https://doi.org/10.1111/1752-1688.12871>, 2020.

733 Heine, R. A., Lant, C. L., and Sengupta, R. R.: Development and comparison of approaches
734 for automated mapping of stream channel networks. *Annals of the Association of*
735 *American Geographers*, 94(3), 477–490. [https://doi.org/10.1111/j.1467-](https://doi.org/10.1111/j.1467-8306.2004.00409.x)
736 [8306.2004.00409.x](https://doi.org/10.1111/j.1467-8306.2004.00409.x), 2004.

737 Hengl, T., Heuvelink, G. B. M. M., and Van Loon, E. E.: On the uncertainty of stream
738 networks derived from elevation data: the error propagation approach. *Hydrology*
739 and *Earth System Sciences*, 14(7), 1153–1165. [https://doi.org/10.5194/hess-14-](https://doi.org/10.5194/hess-14-1153-2010)
740 [1153-2010](https://doi.org/10.5194/hess-14-1153-2010), 2010.

741 Henkle, J. E., Wohl, E., and Beckman, N.: Locations of channel heads in the semiarid
742 Colorado Front Range, USA. *Geomorphology*, 129(3–4), 309–319.
743 <https://doi.org/10.1016/j.geomorph.2011.02.026>, 2011.

Code de champ modifié

Code de champ modifié

Code de champ modifié

Code de champ modifié

744 Horton, B. Y. R. E.: Erosional development of streams and their drainage basins;
745 Hydrophysical approach to quantitative morphology. *GSA Bulletin*, 56(3), 275–
746 370. [https://doi.org/10.1130/0016-7606\(1945\)56\[275:EDOSAT\]2.0.CO;2](https://doi.org/10.1130/0016-7606(1945)56[275:EDOSAT]2.0.CO;2), 1945.

747 James, L. A., Hunt, K. J., Winter, S. W., James, L. A., and Hunt, K. J.: The LiDAR-side of
748 Headwater Streams : Mapping Channel Networks with High-resolution
749 Topographic Data. *Southeastern Geographer*, 50(4), 523–539.
750 <https://doi.org/10.1353/sgo.2010.0009>, 2010.

751 James, L. A., Watson, D. G., and Hansen, W. F.: Using LiDAR data to map gullies and
752 headwater streams under forest canopy: South Carolina, USA. *Catena*, 71(1), 132–
753 144. <https://doi.org/10.1016/j.catena.2006.10.010>, 2007.

754 Jensen, C. K., McGuire, K. J., McLaughlin, D. L., and Scott, D. T.: Quantifying
755 spatiotemporal variation in headwater stream length using flow intermittency
756 sensors. *Environmental Monitoring and Assessment*, 191, 226.
757 <https://doi.org/10.1007/s10661-019-7373-8>, 2019.

758 Jensen, C. K., McGuire, K. J., Shao, Y., and Andrew Dolloff, C.: Modeling wet headwater
759 stream networks across multiple flow conditions in the Appalachian Highlands.
760 *Earth Surface Processes and Landforms*, 43(13), 2762–2778.
761 <https://doi.org/10.1002/esp.4431>, 2018.

762 Jenson, S. K., and Dominique, J. O.: Extracting topographic structure from digital elevation
763 data for geographic information system analysis. *Photogrammetric Engineering*
764 *and Remote Sensing*, 54(11), 1593–1600. 1988.

765 Julian, J. P., Elmore, A. J., and Guinn, S. M.: Channel head locations in forested watersheds
766 across the mid-Atlantic United States: A physiographic analysis. *Geomorphology*,

Code de champ modifié

Code de champ modifié

Code de champ modifié

Code de champ modifié

Code de champ modifié

767 177–178, 194–203. <https://doi.org/10.1016/j.geomorph.2012.07.029>, 2012.

768 Leboeuf, A., and Pomerleau, I.: Projet d'acquisition de données par le capteur LiDAR à
769 l'échelle provinciale : analyse des retombées et recommandations. Ministère des
770 Forêts, de la Faune et des Parcs, Direction des inventaires forestiers. 15 pp., 2015.

771 Leopold, L. B., Wolman, M. G., and Miller, J. P.: Fluvial Processes in Geomorphology.
772 San Francisco, California, W. H. Freeman and Company, 522 pp., 1964.

773 Lessard, F. Optimisation cartographique de l'hydrographie linéaire fine. Master thesis.
774 Department of Wood and Forest Science. Université Laval. 89 pp., 2020.

775 Lessard, F., Jutras, S., Perreault, N., and Guilbert, E.: Performance of automated
776 geoprocessing methods for culvert detection in remote forest environments.
777 Canadian Water Resources Journal,
778 <https://doi.org/10.1080/07011784.2022.2160660>, 2023.

779 Li, R., Tang, Z., Li, X., and Winter, J. Drainage Structure Datasets and Effects on LiDAR-
780 Derived Surface Flow Modeling. ISPRS International Journal of Geo-Information,
781 2(4), 1136–1152. <https://doi.org/10.3390/ijgi2041136>, 2013.

782 Lindsay, J. B.: Sensitivity of channel mapping techniques to uncertainty in digital elevation
783 data. International Journal of Geographical Information Science, 20(6), 669–692.
784 <https://doi.org/10.1080/13658810600661433>, 2006.

785 Lindsay, J. B.: « Whitebox GAT: A Case Study in Geomorphometric Analysis ».
786 Computers and Geosciences 95: 75-84.
787 <https://doi.org/10.1016/j.cageo.2016.07.003>, 2016a.

788 Lindsay, J. B.: Efficient hybrid breaching-filling sink removal methods for flow path
789 enforcement in digital elevation models. Hydrological Processes, 30(6), 846-857.

Code de champ modifié

Code de champ modifié

Code de champ modifié

Code de champ modifié

790 <https://doi.org/10.1002/hyp.10648>, 2016b.

791 Lindsay, J. B., and Dhun, K.: Modelling surface drainage patterns in altered landscapes
792 using LiDAR. *International Journal of Geographical Information Science*, 29(3),
793 397–411. <https://doi.org/10.1080/13658816.2014.975715>, 2015.

794 Meyer, J. L., Strayer, D. L., Wallace, J. B., Eggert, S. L., Helfman, G. S., and Leonard, N.
795 E.: The contribution of headwater streams to biodiversity in river networks. *Journal*
796 *of the American Water Resources Association*, 43(1), 86–103.
797 <https://doi.org/10.1111/j.1752-1688.2007.00008.x>, 2007.

798 Ministère de l'Environnement et de la Lutte contre les changements climatiques
799 (MELCC): Normales climatiques du Québec 1981-2010. [data set].
800 <https://www.environnement.gouv.qc.ca/climat/normales/>, 2022.

801 Montgomery, D. R., and Dietrich, W. E.: Channel Initiation and the Problem of Landscape
802 Scale. *Science*, 255(5046), 826–830.
803 <https://doi.org/10.1126/science.255.5046.826>, 1992.

804 Montgomery, D. R., and Dietrich, W. E.: Landscape dissection and drainage area-slope
805 thresholds. In: Kirkby, M.J. (Ed.), *Process Models and Theoretical*
806 *Geomorphology*. John Wiley and Sons, 221–246. 1994.

807 Montgomery, D. R., and Foufoula-Georgiou, E.: Channel Network Source Representation
808 Using Digital Elevation Models. *Water Resources Research*, 29(12), 3925–3934.
809 <https://doi.org/10.1029/93WR02463>, 1993.

810 Moussa, R., Voltz, M., and Andrieux, P.: Effects of the spatial organization of agricultural
811 management on the hydrological behaviour of a farmed catchment during flood
812 events. *Hydrological Processes*, 16(2), 393–412. <https://doi.org/10.1002/hyp.333>,

Code de champ modifié

Code de champ modifié

Code de champ modifié

Code de champ modifié

Code de champ modifié

Code de champ modifié

Code de champ modifié

813 2002.

814 Murphy, P. N. C., Ogilvie, J. and Arp, P. A.: Topographic modelling of soil moisture
815 conditions: a comparison and verification of two models. European Journal of Soil
816 Science, 60(1), 94-109. <https://doi.org/10.1111/j.1365-2389.2008.01094.x>, 2009.
817 Murphy, P. N. C., Ogilvie, J., Meng, F.-R. R., and Arp, P. A.: Stream network modelling
818 using lidar and photogrammetric digital elevation models: a comparison and field
819 verification. Hydrological Processes, 22(12), 1747-1754.
820 <https://doi.org/10.1002/hyp.6770>, 2008.

821 O'Callaghan, J. F., and Mark, D. M.: The extraction of drainage networks from digital
822 elevation data. Computer Vision, Graphics, and Image Processing, 28(3), 323–344.
823 [https://doi.org/10.1016/S0734-189X\(84\)80011-0](https://doi.org/10.1016/S0734-189X(84)80011-0), 1984.

824 O'Neil, G., and Shortridge, A.: Quantifying local flow direction uncertainty. International
825 Journal of Geographical Information Science, 27(7), 1292–1311.
826 <https://doi.org/10.1080/13658816.2012.719627>, 2013

827 Passalacqua, P., Belmont, P., and Fofoula-Georgiou, E.: Automatic geomorphic feature
828 extraction from lidar in flat and engineered landscapes. Water Resources Research,
829 48(3), 1–18. <https://doi.org/10.1029/2011WR010958>, 2012.

830 Persendt, F. C., and Gomez, C.: Assessment of drainage network extractions in a low-relief
831 area of the Cuvelai Basin (Namibia) from multiple sources: LiDAR, topographic
832 maps, and digital aerial orthophotographs. Geomorphology, 260, 32–50.
833 <https://doi.org/10.1016/j.geomorph.2015.06.047>, 2016.

834 Peucker, T. K., and Douglas, D. H.: Detection of Surface-Specific Points by Local Parallel
835 Processing of Discrete Terrain Elevation Data. Computer Graphics and Image

Code de champ modifié

Code de champ modifié

Code de champ modifié

Code de champ modifié

Code de champ modifié

836 Processing, 4(4), 375–387. [https://doi.org/10.1016/0146-664x\(75\)90005-2](https://doi.org/10.1016/0146-664x(75)90005-2), 1975.

Code de champ modifié

837 [Richardson, M. and Millard, K.: Geomorphic and Biophysical Characterization of Wetland](#)
838 [Ecosystems with Airborne LiDAR Concepts, Methods, and a Case Study. High](#)
839 [Spatial Resolution Remote Sensing 1st Edition, CRC Press, 39 pp. ISBN:](#)
840 [9780429470196, 2018.](#)

841 Roelens, J., Rosier, I., Dondeyne, S., Van Orshoven, J., and Diels, J.: Extracting drainage
842 networks and their connectivity using LiDAR data. *Hydrological Processes*, 32(8),
843 1026–1037. <https://doi.org/10.1002/hyp.11472>, 2018.

844 [Sanders, K. E., Smiley Jr., P. C., Gillespie, R. B., King, K. W., Smith, D. R., and Pappas,](#)
845 [E. A.: Conservation implications of fish–habitat relationships in channelized](#)
846 [agricultural headwater streams. *Journal of Environmental Quality*, 49\(6\), 1585-](#)
847 [1598. <https://doi.org/10.1002/jeq2.20137>, 2020.](#)

a mis en forme : Anglais (Canada)

a mis en forme : Anglais (Canada)

a mis en forme : Français (Canada)

a mis en forme : Français (Canada)

a mis en forme : Français (Canada)

848 Saucier, J.-P., Berger, J.-P., D'Avignon, H., and Racine, P.: Le point d'observation
849 écologique. Ministère des Ressources naturelles, Direction de la gestion des stocks
850 forestiers, Service des inventaires forestiers. 116 pp., 1994.

851 Schwanghart, W., and Heckmann, T.: Fuzzy delineation of drainage basins through
852 probabilistic interpretation of diverging flow algorithms. *Environmental Modelling*
853 and Software, 33, 106–113. <https://doi.org/10.1016/j.envsoft.2012.01.016>, 2012.

Code de champ modifié

854 St-Hilaire, A., Duchesne, S., and Rousseau, A. N.: Floods and water quality in Canada: A
855 review of the interactions with urbanization, agriculture and forestry. *Canadian*
856 *Water Resources Journal*, 41(1–2), 273–287.
857 <https://doi.org/10.1080/07011784.2015.1010181>, 2016.

Code de champ modifié

858 Tribe, A.: Automated recognition of valley lines and drainage networks from grid digital

859 elevation models: a review and a new method. *Journal of Hydrology*, 139(1–4),
860 263–293. [https://doi.org/10.1016/0022-1694\(92\)90206-B](https://doi.org/10.1016/0022-1694(92)90206-B), 1992.

861 Tucker, G. E., and Slingerland, R.: Predicting sediment flux from fold and thrust belts.
862 *Basin Research*, 8(3), 329–349. <https://doi.org/10.1046/j.1365-2117.1996.00238.x>,
863 1996.

864 Van Meerveld, H. J. I., Kirchner, J. W., Vis, M. J. P., Assendelft, R. S., and Seibert, J.:
865 Expansion and contraction of the flowing stream network changes hillslope
866 flowpath lengths and the shape of the travel time distribution. *Hydrology and Earth
867 System Sciences*, 23(11), 4825–4834. <https://doi.org/10.5194/hess-23-4825-2019>,
868 2019.

869 Wechsler, S. P.: Uncertainties associated with digital elevation models for hydrologic
870 applications: a review. *Hydrology and Earth System Sciences*, 11(4), 1481–1500.
871 <https://doi.org/10.5194/hess-11-1481-2007>, 2007.

872 Weiss, A.: Topographic position and landforms analysis. Poster Presentation, ESRI User
873 Conference, San Diego, California. USA. 2001.

874 White, B., Ogilvie, J., Campbell, D. M. H., Hiltz, D., Gauthier, B., Chisholm, H. K. H.,
875 Wen, H. K., Murphy, P. N. C., and Arp, P. A.: Using the Cartographic Depth-to-
876 Water Index to Locate Small Streams and Associated Wet Areas across
877 Landscapes. *Canadian Water Resources Journal*, 37(4), 333–347.
878 <https://doi.org/10.4296/cwrj2011-909>, 2012.

879 Wohl, E.: The challenges of channel heads. *Earth-Science Reviews*, 185, 649–664.
880 <https://doi.org/10.1016/j.earscirev.2018.07.008>, 2018.

881 Wu, J., Liu, H., Wang, Z., Ye, L., Li, M., Peng, Y., Zhang, C., and Zhou, H.: Channel head

Code de champ modifié

Code de champ modifié

Code de champ modifié

Code de champ modifié

Code de champ modifié

Code de champ modifié

882 extraction based on fuzzy unsupervised machine learning method. *Geomorphology*,
883 391, 107888. <https://doi.org/10.1016/j.geomorph.2021.107888>, 2021.

884 Wulder, M. A., Bater, C. W., Coops, N. C., Hilker, T., White, J. C.: The role of LiDAR in
885 sustainable forest management. *Forestry Chronicle*, 84(6), 807–826.
886 <https://doi.org/10.5558/tfc84807-6>, 2008.

Code de champ modifié